



HHS Public Access

Author manuscript

Prostaglandins Other Lipid Mediat. Author manuscript; available in PMC 2019 July 06.

Published in final edited form as:

Prostaglandins Other Lipid Mediat. 2018 July ; 137: 63–68. doi:10.1016/j.prostaglandins.2018.07.001.

The contribution of TRPV1 channel to 20-HETE–aggravated ischemic neuronal injury

Xiaofan Zhang^{1,2,3}, Nagat El Demerdash¹, John R. Falck⁴, Sailu Munnuri⁴, Raymond C. Koehler¹, and Zeng-Jin Yang¹

¹Department of Anesthesiology/Critical Care Medicine, Johns Hopkins University, Baltimore, Maryland. ²State Key Laboratory of Freshwater Ecology and Biotechnology, Institute of Hydrobiology, Chinese Academy of Sciences, Wuhan, Hubei, China. ³University of Chinese Academy of Sciences, Beijing, China. ⁴Department of Biochemistry, University of Texas Southwestern Medical Center, Dallas, Texas

Abstract

20-Hydroxyeicosatetraenoic acid (20-HETE), a cytochrome P450 (CYP) 4A/4F-derived metabolite of arachidonic acid, directly contributes to ischemic neuronal injury. However, little is known about mediators of 20-HETE neurotoxicity after ischemia. Here, we focus on the role of transient receptor potential cation channel subfamily V member 1 (TRPV1) in 20-HETE-induced neurotoxicity. Our results showed that TRPV1 and CYP4A immunoreactivity were colocalized in neurons. TRPV1 inhibition attenuated 20-HETE mimetic 20-5,14-HEDGE-induced reactive oxygen species (ROS) production and neuronal injury in cultured neurons and protected ischemic neurons *in vitro* and *in vivo*. TRPV1 inhibition in combination with 20-HETE synthesis inhibitor HET0016 did not produce additional protective effects. Furthermore, TRPV1 genetic inhibition and NADPH oxidase inhibitor gp91ds-dat each attenuated ROS production to a similar extent. However, combined treatment did not achieve additional reduction. Therefore, we conclude that TRPV1 channels are involved in 20-HETE's ROS generation and neurotoxicity after ischemia.

Keywords

20-HETE; TRPV1; Oxygen-glucose deprivation; Hypoxic-ischemic injury; Neonatal

* **Corresponding author:** Zeng-Jin Yang, MD, PhD, Department of Anesthesiology and Critical Care Medicine, Johns Hopkins University, 720 Rutland Ave, Traylor 804, Baltimore, MD 21205, USA. zyang4@ihmi.edu.

AUTHOR CONTRIBUTIONS

X.Z., N.E.D., and Z.-J.Y. performed the experiments. R.C.K. and Z.-J.Y. conceived and designed the experiments and analyzed the data. J.R.F. and S.M. provided 20-HETE agonist. J.R.F. and R.J.R. provided oversight for the project. R.C.K. and Z.-J.Y. compiled the manuscript and figure preparation.

CONFLICTS OF INTEREST

The authors declare no conflicts of interest.

Publisher's Disclaimer: This is a PDF file of an unedited manuscript that has been accepted for publication. As a service to our customers we are providing this early version of the manuscript. The manuscript will undergo copyediting, typesetting, and review of the resulting proof before it is published in its final form. Please note that during the production process errors may be discovered which could affect the content, and all legal disclaimers that apply to the journal pertain.

1. INTRODUCTION

20-Hydroxyeicosatetraenoic acid (20-HETE) is a cytochrome P450 (CYP) 4A/4F-derived metabolite of arachidonic acid [1]. 20-HETE is elevated in cerebrospinal fluid and plasma of stroke patients with poor outcomes [2, 3]. Moreover, 20-HETE synthesis inhibitors provide substantial neuroprotection in adult and newborn brain ischemia models [4-9]. Therefore, 20-HETE plays critical roles in the pathophysiologic process of brain ischemia. Although 20-HETE is well known for its vascular effects [10], our studies and those of others suggest that these inhibitors do not affect pial artery diameter or cerebral blood flow during the ischemic period [4, 7, 9, 11]. Renic et al. reported that an inhibitor of 20-HETE synthesis protected organotypic hippocampal slice cultures from oxygen-glucose deprivation (OGD) [7], which suggested that 20-HETE had direct effects on brain parenchyma after ischemia. Our recent work [12] further showed that primary neurons express Cyp4a10 and 4a12a, the specific CYP4A members known to synthesize 20-HETE in mice [13]. We also found that the 20-HETE agonist 20-5,14-HEDGE leads to reactive oxygen species (ROS) production in cultured neurons, whereas neuronally derived 20-HETE after OGD directly contributes to ROS generation and neuronal death after reoxygenation. Therefore, 20-HETE may directly promote neuronal damage after ischemia. However, little is known about the downstream molecular signaling involved in 20-HETE's direct neurotoxicity after ischemia.

Transient receptor potential cation channel subfamily V member 1 (TRPV1), the nonselective cation channel with massive Ca^{2+} permeability, is widely distributed in the brain [14]. TRPV1 activation not only increases ROS generation [15], but can also cause significant neuronal injury [16-18]. More importantly, it interacts with 20-HETE in neural and non-neural tissues. For example, 20-HETE activates TRPV1 in dorsal root ganglion neurons [19, 20], and the specific TRPV1 antagonist capsazepine abolishes 20-HETE-induced tonic response in airway smooth muscle [21]. However, the relationship between TRPV1 and 20-HETE after ischemia is unclear. Therefore, in the present study, we used *in vitro* and *in vivo* brain ischemia models to study whether TRPV1 channels are involved in 20-HETE's direct neurotoxicity.

2. MATERIALS AND METHODS

2.1 Animal and reagents

C57Bl/6 and TRPV1 knockout (KO) mice (C57Bl/6 background) were purchased from the Jackson Laboratory (Bar Harbor, ME). The ω -hydroxylase inhibitor N-hydroxy-N'-(4-n-butyl-2-methylphenyl)formamidinium (HET0016) was purchased from Enzo (Farmingdale, NY). A784168 was purchased from Tocris (Minneapolis, MN). gp91 ds-tat and gp91 ds-tat scrambled were purchased from AnaSpec (Fremont, CA). The 20-HETE stable agonist N-(20-hydroxyeicosa-5[Z],14[Z]-dienoyl)glycine (20-5,14-HEDGE) was synthesized in the laboratory of J.R. Falck.

2.2 Mouse hypoxic-ischemic (H-I) brain injury

The animal protocols complied with the ARRIVE guidelines (<https://www.nc3rs.org.uk/arrive-guidelines>), were approved by the Animal Care and Use Committee of the Johns

Hopkins University, and were carried out with standards of care and housing in accordance with the National Institutes of Health *Guide for the Care and Use of Laboratory Animals*. Animals from each litter were randomized to sham or H-I procedure. Hypoxia-ischemia was induced with an adaptation of the Vannucci procedure [22]. In brief, mice on postnatal day 10 were anesthetized with isoflurane (2% isoflurane/balance oxygen for induction and 1% for maintenance) and the left carotid artery was ligated. Pups were allowed to recover for 2 h with the dam after surgery before being exposed for 45 min to a humidified mixture of 8% oxygen (balance nitrogen) in enclosed, vented chambers submerged in a 37.0°C water bath. Animals then recovered for 15 min in a temperature-controlled incubator set to an ambient temperature of 37.0°C and were returned to their dams until sacrifice. Sham-operated animals received isoflurane anesthesia and exposure of the left common carotid artery without ligation or hypoxia. Animals were injected intraperitoneally vehicle (0.1% DMSO in 0.9% normal saline), TRPV1 specific inhibitor A784168 (10 µmol/kg), or/and 20-HETE synthesis inhibitor HET0016 (1 mg/kg) 15 min before H-I. Brains were removed at 24 h after H-I induction or control procedure, sliced coronally into 2-mm-thick sections, and stained with 0.5% 2,3,5-triphenyltetrazolium chloride (TTC) for infarct volume measurement.

2.3 Cortical neuron culture and OGD

Procedures used for neuronal culture and OGD have been described previously [12]. In brief, cerebrocortical cells were isolated from cerebral cortex of mice on embryonic day 17 and plated with Neurobasal medium supplemented with B27, glutamine, and streptomycin/penicillin (ThermoFisher, Grand Island, NY) onto culture plates coated with poly-D-lysine (MilliporeSigma, St. Louis, MO). The procedure yielded cell cultures with approximately 90% neurons, as determined by NeuN staining. Cells at 7–9 days *in vitro* were used for OGD or pharmacologic treatment. For OGD, neurons were incubated in glucose-free Neurobasal medium with B27 minus antioxidants (ThermoFisher) in a chamber filled with 5% CO₂ and 95% N₂ at 37 °C for 1 h. Control cells were incubated in normal culture medium in a normoxic incubator for the same period. OGD was terminated by switching back to normal culture conditions with glucose. We measured the effects of the 20-HETE synthesis inhibitor HET0016 (10 µM), TRPV1 antagonist A784168 (1, 10, or 50 µM), the NOX2-specific inhibitor gp91ds-tat (0.1, 1, or 5 µM), and 20-HETE agonist 20-5,14-HEDGE (10 µM) on cell survival by adding the compound or vehicle (0.1% DMSO) to the cell culture medium for 15 min before and 1 h during exposure to OGD. Cell viability was assessed with the CellTiter-Blue cell viability assay (Promega, Madison, WI) at 24 h after OGD. At least three independent experiments were performed for each intervention.

2.4 Immunohistochemistry and immunocytochemistry

Anesthetized 10-day-old C57Bl/6 mice were perfused with phosphate-buffered saline (PBS) and 4% paraformaldehyde. Brains were collected and cut into 40-µm-thick frozen sections. The sections were blocked with 10% normal serum and incubated with rabbit anti-cytochrome P450 4A (CYP4A) antibody (1:300; ab3573, Abcam, Cambridge, MA) or mouse anti-NeuN (1:500, MAB377, MilliporeSigma) and mouse anti-VR1 (1:300, sc-398417, Santa Cruz Biotechnology, Dallas, TX) overnight at 4 °C, followed by 1-h incubation with anti-IgG antibodies conjugated with Alexa Fluor 488 or 594 (1:1000, ThermoFisher).

Paraformaldehyde-fixed cells (on glass coverslips) were washed with PBS, permeabilized with 0.1% Triton X-100 (MilliporeSigma), blocked for 30 min with 10% normal goat serum in PBS, and incubated with rabbit anti-CYP4A antibody and mouse anti-VR1 antibody overnight at 4 °C, followed by 1-h incubation with anti-rabbit or anti-mouse IgG antibodies conjugated with Alexa Fluor 488 or 594.

2.5 Quantitative reverse transcriptase PCR (qPCR)

RNA was extracted from brain tissues, and qPCR was used to quantify the mRNA of CYP4A isoforms in C57Bl/6 and TRPV1 KO mice, as described previously [12].

2.6 Oxidative stress measurement

ROS formation in cultured neurons was measured with a 2',7'-dichlorodihydrofluorescein diacetate (DCFDA) cellular ROS detection assay kit (ab113851, Abcam), as described previously [12]. Oxidative modification of proteins in the ipsilateral hemisphere after H-I was determined with an OxyBlot protein oxidation detection kit (MilliporeSigma) for carbonyl groups as described [9]. Glyceraldehyde 3-phosphate dehydrogenase (GAPDH; 1:2000, ab9485, Abcam) was used as loading control.

2.7 Statistical analysis

All data are expressed as mean \pm standard deviation and analyzed by one-way ANOVA followed by the Student–Newman–Keuls multiple test. A value of $p < 0.05$ was considered statistically significant.

3. RESULTS

3.1 TRPV1 and CYP4A in neurons

TRPV1 immunoreactivity were widely distributed in cortical neurons *in vitro* and *in vivo* (Fig. 1). This finding is consistent with previous reports of cortical TRPV1 expression [17, 23]. Moreover, CYP4A and TRPV1 signals co-localized in cultured neurons and cerebral cortical neurons of 10-day-old mice.

3.2 Roles of TRPV1 and 20-HETE in OGD neurons

One-hour OGD led to neuronal injury at 24 h of reoxygenation. The injury was attenuated to similar extents by 10 and 50 μ M of the TRPV1 antagonist A784168 (Fig. 2A). Thus, we used 10 μ M A784168 in the following experiments to validate the neuroprotective effects of pharmacologic TRPV1 inhibition. Further analysis indicated that A784168 and 10 μ M HET0016 treatment produced comparable protection against 1-h OGD-induced neuronal injury (Fig. 2B). Similar neuroprotection also was found in TRPV1 KO neurons (Fig. 2C). A combination of TRPV1 pharmacologic or genetic inhibition and HET0016 did not produce additional protection against OGD injury.

3.3 Roles of TRPV1 and 20-HETE in newborn H-I brains

Unilateral carotid artery ligation followed by 45 min of hypoxia produced ipsilateral brain injury in newborn mice (Fig. 2D). Individually, TRPV1 genetic inhibition and pretreatment

with 10 $\mu\text{mol/kg}$ A784168 or 1 mg/kg HET0016 (i.p. 15 min before H-I) attenuated brain injury to a similar extent at 1 day after H-I. Combining A784168 and HET0016, however, did not provide additional protection.

3.4 TRPV1, 20-HETE, and ROS after OGD or H-I

20-HETE mimetic 20-5,14-HEDGE shows improved stability *in vitro* compared to 20-HETE, due to its glycine substitution and absence of double bonds preventing its degradation by β -oxidation and cyclooxygenase [24]. One-hour treatment with 20-5,14-HEDGE induced ROS generation in cultured neurons without OGD injury (Fig. 3A) that was attenuated in TRPV1 KO neurons and by treatment of wild-type (WT) neurons with A784168 or HET0016. HET0016 and A784168 in combination, however, did not provide additive effects. One-hour OGD produced massive ROS at 1 h of reoxygenation (Fig. 3B). HET0016 and A784168 each reduced H-I-induced ROS production, but the drug combination did not provide extra ROS inhibition.

Protein carbonyl formation is used as a marker of oxidative stress [25]. Oxyblot analysis of carbonyl groups indicated that total tissue lysates of the ipsilateral hemisphere were significantly increased at 3 h of recovery from H-I (Fig. 3C). HET0016 and A784168 significantly lessened carbonyl formation. The combination of HET0016 and A784168 did not provide additional reduction.

3.5 Effect of TRPV1 knockout on CYP4A mRNA and body temperature

The mRNA levels for Cyp4a10 and Cyp4a12a in brain tissue did not differ significantly between TRPV1 KO and C57Bl/6 WT mice (Fig. 4A). TRPV1 channels in hypothalamus have been implicated in temperature regulation [26]. However, we found that adult TRPV1 KO and C57Bl/6 mice showed comparable baseline rectal temperature and a similar anesthesia-induced temperature decrease without external warming. A784168 increased body temperature only transiently (Fig. 4B).

3.6 TRPV1, NOX2, and ROS production

20-HETE promotes the assembly of NADPH oxidase 2 (NOX2) and increases ROS production in non-neuronal cells [27, 28]. Here, we used the NOX2-specific inhibitor gp91ds-dat to determine whether NOX2 plays any role in 20-HETE-induced ROS generation in neurons. 20-5,14-HEDGE induced an increase in ROS generation equivalent to 440% of vehicle, but this increase was reduced to 270%, 200%, and 200% with the application of 0.1, 1, and 5 μM gp91ds-tat, respectively. The scrambled gp91 ds-tat did not affect ROS induction (Fig. 5A). TRPV1 knockout attenuated ROS production to a similar extent as 1 μM gp91ds-tat. Administration of gp91ds-tat to TRPV1 KO neurons, however, did not result in greater ROS reduction (Fig. 5B).

4 DISCUSSION

Our work indicates that the TRPV1 channel contributes to 20-HETE-induced neurotoxicity. We found that (1) TRPV1 and CYP4A immunoreactivity co-localize in primary cortical neurons and neuron-like cells in cerebral cortex of newborn mice; (2) pharmacologic or

genetic TRPV1 inhibition attenuated 20-HETE-aggravated neuronal injury after OGD or H-I; (3) pharmacologic or genetic TRPV1 inhibition attenuated 20-HETE mimetic-induced ROS production and 20-HETE-aggravated ROS generation after OGD; (4) pharmacologic TRPV1 inhibition reduced H-I-induced carbonyl formation in ipsilateral brain tissues; and (5) application of a NOX2-specific inhibitor attenuated 20-HETE mimetic-induced ROS production, but this protection was not additive with TRPV1 genetic inhibition.

TRPV1 channels modulate temperature regulation [26]. Hence, TRPV1 agonists could induce hypothermia that, in turn, protects ischemic brains [29, 30]. Nevertheless, our studies showed that TRPV1 KO mice have a normal body temperature, as reported in previous work [31-33]. Furthermore, the hyperthermic action of TRPV1 antagonists can be separated from their other effects [34, 35]. Here, 10 $\mu\text{mol/kg}$ A784168 produced only brief hyperthermia in normal anesthetized mice. Therefore, neither A784168 nor TRPV1 knockout is likely to cause significant temperature change, and body temperature changes are unlikely to account for TRPV1's neuroprotective effects.

Furthermore, we do not know whether 20-HETE directly binds to TRPV1 or works through other molecules to activate TRPV1. In addition, we cannot exclude the possibility that 20-5,14-HEDGE, with its slightly altered chemical structure and long half-life, will exert a more sustained and different effect on target receptors or ligands than the short-lived 20-HETE molecule. Although our work shows that TRPV1 mediates 20-HETE toxicity, 20-HETE may serve as an intracellular secondary messenger to directly activate PKC and G proteins [1], which may affect neuronal fate after ischemia. In addition, other 20-HETE mediators/receptors might play roles after ischemia. For example, GPR75 is the first 20-HETE receptor to be identified in endothelial cells [36]. Whether GPR75 plays a role in 20-HETE neuronal toxicity requires further work. Lastly, our results do not address the role of 20-HETE/TRPV1 signal coupling under normal physiologic conditions in neurons. We did not observe an effect of the TRPV1 antagonist or the 20-HETE synthesis inhibitor on ROS detection with DCFDA in the absence of OGD (Fig. 3A), but our whole-well neuronal cell measurement was not designed for detecting physiologic ROS signaling in a subcellular compartment in quiescent neurons in culture.

Collectively, our findings indicate that TRPV1 channels are involved in 20-HETE-induced oxidative stress and 20-HETE-aggravated neuronal injury *in vitro* and *in vivo*. Inhibition of TRPV1 has a protective effect against OGD/H-I-induced neuronal injury. In conclusion, these findings suggest that TRPV1 channels contribute to 20-HETE-induced neurotoxicity after ischemia.

ACKNOWLEDGEMENTS

We thank Claire Levine for assistance with manuscript preparation.

FUNDING

X.Z. was supported by a Chinese Scholarship Council student fellowship grant. J.R.F. was supported by National Institutes of Health (NIH) Grant HL139793 and by the Robert A. Welch Foundation (I-0011). R.C.K. was supported by NIH Grants NS060703 and NS067525. Z.J.Y. was supported by a Stimulating and Advancing ACCM Research (StAAR) grant from the Department of Anesthesiology and Critical Care Medicine, Johns Hopkins University.

REFERENCES

- [1]. Roman RJ , P-450 metabolites of arachidonic acid in the control of cardiovascular function, *Physiological reviews* 82(1) (2002) 131–85. [PubMed: 11773611]
- [2]. Yi X , Han Z , Zhou Q , Lin J , Liu P , 20-Hydroxyecosatetraenoic Acid as a Predictor of Neurological Deterioration in Acute Minor Ischemic Stroke, *Stroke* 47(12) (2016) 3045–3047. [PubMed: 27834744]
- [3]. Crago EA , Thampatty BP , Sherwood PR , Kuo CW , Bender C , Balzer J , Horowitz M , Poloyac SM , Cerebrospinal fluid 20-HETE is associated with delayed cerebral ischemia and poor outcomes after aneurysmal subarachnoid hemorrhage, *Stroke* 42(7) (2011) 1872–7. [PubMed: 21617146]
- [4]. Cao S , Wang LC , Kwansa H , Roman RJ , Harder DR , Koehler RC , Endothelin rather than 20-HETE contributes to loss of pial arteriolar dilation during focal cerebral ischemia with and without polymeric hemoglobin transfusion, *American journal of physiology. Regulatory, integrative and comparative physiology* 296(5) (2009) R1412–8.
- [5]. Kawasaki T , Marumo T , Shirakami K , Mori T , Doi H , Suzuki M , Watanabe Y , Chaki S , Nakazato A , Ago Y , Hashimoto H , Matsuda T , Baba A , Onoe H , Increase of 20-HETE synthase after brain ischemia in rats revealed by PET study with 11C-labeled 20-HETE synthase-specific inhibitor, *J Cereb Blood Flow Metab* 32(9) (2012) 1737–46. [PubMed: 22669478]
- [6]. Marumo T , Eto K , Wake H , Omura T , Nabekura J , The inhibitor of 20-HETE synthesis, TS-011, improves cerebral microcirculatory autoregulation impaired by middle cerebral artery occlusion in mice, *British journal of pharmacology* 161(6) (2010) 1391–402. [PubMed: 20735406]
- [7]. Renic M , Kumar SN , Gebremedhin D , Florence MA , Gerges NZ , Falck JR , Harder DR , Roman RJ , Protective effect of 20-HETE inhibition in a model of oxygen-glucose deprivation in hippocampal slice cultures, *American journal of physiology. Heart and circulatory physiology* 302(6) (2012) H1285–93. [PubMed: 22245774]
- [8]. Tanaka Y , Omura T , Fukasawa M , Horiuchi N , Miyata N , Minagawa T , Yoshida S , Nakaike S , Continuous inhibition of 20-HETE synthesis by TS-011 improves neurological and functional outcomes after transient focal cerebral ischemia in rats, *Neurosci Res* 59(4) (2007) 475–80. [PubMed: 17933409]
- [9]. Yang ZJ , Carter EL , Kibler KK , Kwansa H , Crafa DA , Martin LJ , Roman RJ , Harder DR , Koehler RC , Attenuation of neonatal ischemic brain damage using a 20-HETE synthesis inhibitor, *J Neurochem* 121(1) (2012) 168–79. [PubMed: 22251169]
- [10]. Hoopes SL , Garcia V , Edin ML , Schwartzman ML , Zeldin DC , Vascular actions of 20-HETE, *Prostaglandins Other Lipid Mediat* 120 (2015) 9–16. [PubMed: 25813407]
- [11]. Renic M , Klaus JA , Omura T , Kawashima N , Onishi M , Miyata N , Koehler RC , Harder DR , Roman RJ , Effect of 20-HETE inhibition on infarct volume and cerebral blood flow after transient middle cerebral artery occlusion, *J Cereb Blood Flow Metab* 29(3) (2009) 629–39. [PubMed: 19107134]
- [12]. Zhang H , Falck JR , Roman RJ , Harder DR , Koehler RC , Yang ZJ , Upregulation of 20-HETE Synthetic Cytochrome P450 Isoforms by Oxygen-Glucose Deprivation in Cortical Neurons, *Cell Mol Neurobiol* (2017).
- [13]. Muller DN , Schmidt C , Barbosa-Sicard E , Wellner M , Gross V , Hercule H , Markovic M , Honeck H , Luft FC , Schunck WH , Mouse Cyp4a isoforms: enzymatic properties, gender- and strain-specific expression, and role in renal 20-hydroxyecosatetraenoic acid formation, *The Biochemical journal* 403(1) (2007) 109–18. [PubMed: 17112342]
- [14]. Caterina MJ , Julius D , The vanilloid receptor: a molecular gateway to the pain pathway, *Annual review of neuroscience* 24 (2001) 487–517.
- [15]. Ma F , Zhang L , Westlund KN , Reactive oxygen species mediate TNFR1 increase after TRPV1 activation in mouse DRG neurons, *Mol Pain* 5 (2009) 31. [PubMed: 19531269]
- [16]. Kim SR , Lee DY , Chung ES , Oh UT , Kim SU , Jin BK , Transient receptor potential vanilloid subtype 1 mediates cell death of mesencephalic dopaminergic neurons in vivo and in vitro, *J Neurosci* 25(3) (2005) 662–71. [PubMed: 15659603]

- [17]. Song J , Lee JH , Lee SH , Park KA , Lee WT , Lee JE , TRPV1 Activation in Primary Cortical Neurons Induces Calcium-Dependent Programmed Cell Death, *Experimental neurobiology* 22(1) (2013) 51–7. [PubMed: 23585723]
- [18]. Shirakawa H , Yamaoka T , Sanpei K , Sasaoka H , Nakagawa T , Kaneko S , TRPV1 stimulation triggers apoptotic cell death of rat cortical neurons, *Biochemical and biophysical research communications* 377(4) (2008) 1211–5. [PubMed: 18996081]
- [19]. Wen H , Ostman J , Bubb KJ , Panayiotou C , Priestley JV , Baker MD , Ahluwalia A , 20-Hydroxyeicosatetraenoic acid (20-HETE) is a novel activator of transient receptor potential vanilloid 1 (TRPV1) channel, *J Biol Chem* 287(17) (2012) 13868–76. [PubMed: 22389490]
- [20]. Bubb KJ , Wen H , Panayiotou CM , Finsterbusch M , Khan FJ , Chan MV , Priestley JV , Baker MD , Ahluwalia A , Activation of neuronal transient receptor potential vanilloid 1 channel underlies 20-hydroxyeicosatetraenoic acid-induced vasoactivity: role for protein kinase A, *Hypertension* 62(2) (2013) 426–33. [PubMed: 23753406]
- [21]. Rousseau E , Cloutier M , Morin C , Proteau S , Capsazepine, a vanilloid antagonist, abolishes tonic responses induced by 20-HETE on guinea pig airway smooth muscle, *Am J Physiol Lung Cell Mol Physiol* 288(3) (2005) L460–70. [PubMed: 15557084]
- [22]. Rice JE , Vannucci RC , Brierley JB , The influence of immaturity on hypoxic-ischemic brain damage in the rat, *Annals of neurology* 9(2) (1981) 131–41. [PubMed: 7235629]
- [23]. Marrone MC , Morabito A , Giustizieri M , Chiurciu V , Leuti A , Mattioli M , Marinelli S , Riganti L , Lombardi M , Murana E , Totaro A , Piomelli D , Ragozzino D , Oddi S , Maccarrone M , Verderio C , Marinelli S , TRPV1 channels are critical brain inflammation detectors and neuropathic pain biomarkers in mice, *Nature communications* 8 (2017) 15292.
- [24]. Alonso-Galicia M , Falck JR , Reddy KM , Roman RJ , 20-HETE agonists and antagonists in the renal circulation, *Am J Physiol* 277(5 Pt 2) (1999) F790–6. [PubMed: 10564244]
- [25]. Yang ZJ , Carter EL , Torbey M , Martin LJ , Koehler RC , Sigma receptor ligand 4-phenyl-1-(4-phenylbutyl)-piperidine modulates neuronal nitric oxide synthase/postsynaptic density-95 coupling mechanisms and protects against neonatal ischemic degeneration of striatal neurons, *Experimental neurology* 221(1) (2010) 166–174. [PubMed: 19883643]
- [26]. Cavanaugh DJ , Chesler AT , Jackson AC , Sigal YM , Yamanaka H , Grant R , O'Donnell D , Nicoll RA , Shah NM , Julius D , Basbaum AI , Trpv1 reporter mice reveal highly restricted brain distribution and functional expression in arteriolar smooth muscle cells, *J Neurosci* 31(13) (2011) 5067–77. [PubMed: 21451044]
- [27]. Tunctan B , Korkmaz B , Sari AN , Kacan M , Unsal D , Serin MS , Buharalioglu CK , Sahan-Firat S , Cuez T , Schunck WH , Manthathi VL , Falck JR , Malik KU , Contribution of iNOS/sGC/PKG pathway, COX-2, CYP4A1, and gp91(phox) to the protective effect of 5,14-HEDGE, a 20-HETE mimetic, against vasodilation, hypotension, tachycardia, and inflammation in a rat model of septic shock, *Nitric Oxide* 33 (2013) 18–41. [PubMed: 23684565]
- [28]. Medhora M , Chen Y , Gruenloh S , Harland D , Bodiga S , Zielonka J , Gebremedhin D , Gao Y , Falck JR , Anjaiah S , Jacobs ER , 20-HETE increases superoxide production and activates NAPDH oxidase in pulmonary artery endothelial cells, *Am J Physiol Lung Cell Mol Physiol* 294(5) (2008) L902–11. [PubMed: 18296498]
- [29]. Cao Z , Balasubramanian A , Marrelli SP , Pharmacologically induced hypothermia via TRPV1 channel agonism provides neuroprotection following ischemic stroke when initiated 90 min after reperfusion, *American journal of physiology. Regulatory, integrative and comparative physiology* 306(2) (2014) R149–56.
- [30]. Muzzi M , Felici R , Cavone L , Gerace E , Minassi A , Appendino G , Moroni F , Chiarugi A , Ischemic neuroprotection by TRPV1 receptor-induced hypothermia, *J Cereb Blood Flow Metab* 32(6) (2012) 978–82. [PubMed: 22434066]
- [31]. Garami A , Pakai E , Oliveira DL , Steiner AA , Wanner SP , Almeida MC , Lesnikov VA , Gavva NR , Romanovsky AA , Thermoregulatory phenotype of the Trpv1 knockout mouse: thermoeffector dysbalance with hyperkinesis, *J Neurosci* 31(5) (2011) 1721–33. [PubMed: 21289181]
- [32]. Szelenyi Z , Hummel Z , Szolcsanyi J , Davis JB , Daily body temperature rhythm and heat tolerance in TRPV1 knockout and capsaicin pretreated mice, *The European journal of neuroscience* 19(5) (2004) 1421–4. [PubMed: 15016100]

- [33]. Iida T , Shimizu I , Nealen ML , Campbell A , Caterina M , Attenuated fever response in mice lacking TRPV1, *Neuroscience letters* 378(1) (2005) 28–33. [PubMed: 15763167]
- [34]. Nash MS , McIntyre P , Groarke A , Lilley E , Culshaw A , Hallett A , Panesar M , Fox A , Bevan S , 7-tert-Butyl-6-(4-chloro-phenyl)-2-thioxo-2,3-dihydro-1H-pyrido[2,3-d]pyrimidin-4 -one, a classic polymodal inhibitor of transient receptor potential vanilloid type 1 with a reduced liability for hyperthermia, is analgesic and ameliorates visceral hypersensitivity, *J Pharmacol Exp Ther* 342(2) (2012) 389–98. [PubMed: 22566669]
- [35]. Watabiki T , Kiso T , Kuramochi T , Yonezawa K , Tsuji N , Kohara A , Kakimoto S , Aoki T , Matsuoka N , Amelioration of neuropathic pain by novel transient receptor potential vanilloid 1 antagonist AS1928370 in rats without hyperthermic effect, *J Pharmacol Exp Ther* 336(3) (2011) 743–50. [PubMed: 21098091]
- [36]. Garcia V , Gilani A , Shkolnik B , Pandey V , Zhang FF , Dakarapu R , Gandham SK , Reddy NR , Graves JP , Gruzdev A , Zeldin DC , Capdevila JH , Falck JR , Schwartzman ML , 20-HETE Signals Through G-Protein-Coupled Receptor GPR75 (Gq) to Affect Vascular Function and Trigger Hypertension, *Circulation research* 120(11) (2017) 1776–1788. [PubMed: 28325781]

Highlights

- TRPV1 inhibition attenuates 20-HETE-aggravated neuronal injury after OGD or H-I.
- TRPV1 inhibition reduces 20-HETE mimetic-induced ROS production and 20-HETE-aggravated ROS generation after OGD or H-I.
- NOX2 may be involved in TRPV1's roles.

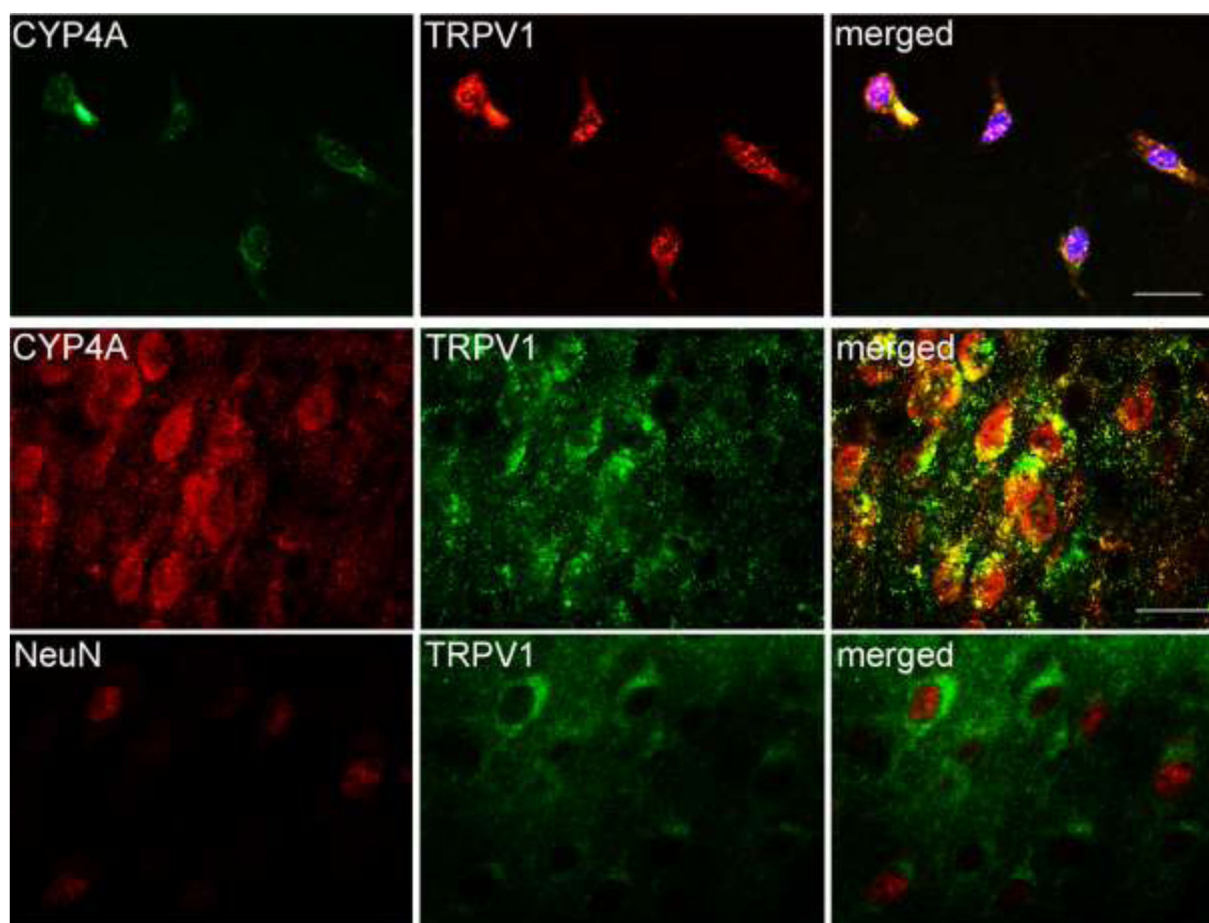
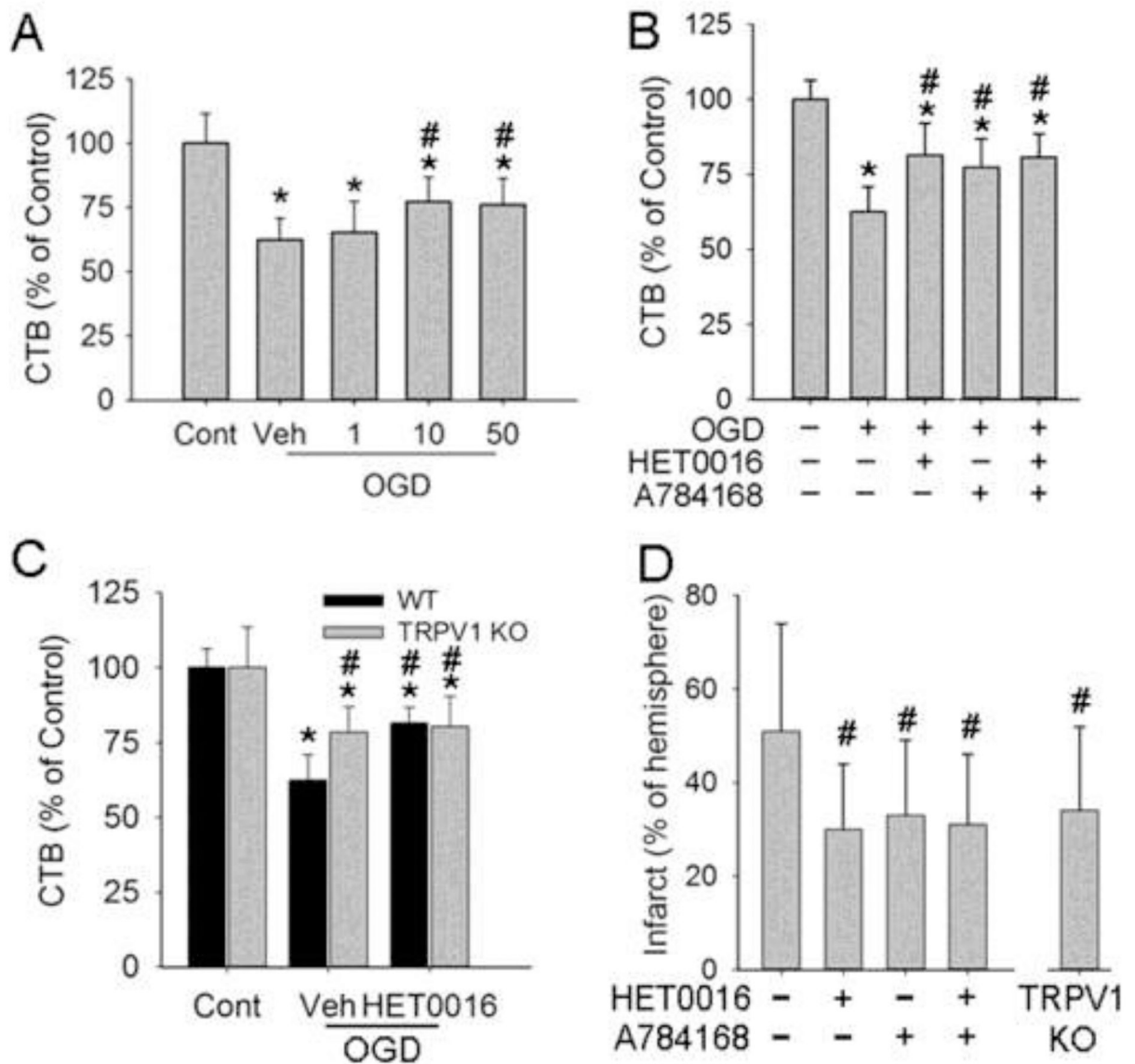


Figure 1. Double immunofluorescent staining indicates that CYP4A and TRPV1 are colocalized in cultured mouse cortical neurons (upper panel) and cerebral cortical neurons of 10-day-old mice (lower panel). DAPI is used to display nuclei of cultured cells. Scale bar = 20 μ m.

**Figure 2.**

Effects of HET0016 and TRPV1 inhibition on neuronal injury. Cell viability was assessed with the CellTiter-Blue assay. (A) TRPV1 inhibitor A784168 at 10 and 50 μ M protected OGD neurons at 24 h of reoxygenation. (B, C) A784168 (10 μ M, B) and TRPV1 genetic knockout (KO, C) each protected neurons from OGD injury. HET0016 did not augment protection. (D) A784168 and HET0016 each attenuated H-I brain injury in newborn mice at 1 day of recovery (n=20-25/group), but did not exhibit additive effects. TRPV1 KO also protected H-I brains at 1 day. * p <0.05 vs wild-type (WT)+control procedure (Cont); # p <0.05 vs WT OGD/H-I+vehicle (Veh).

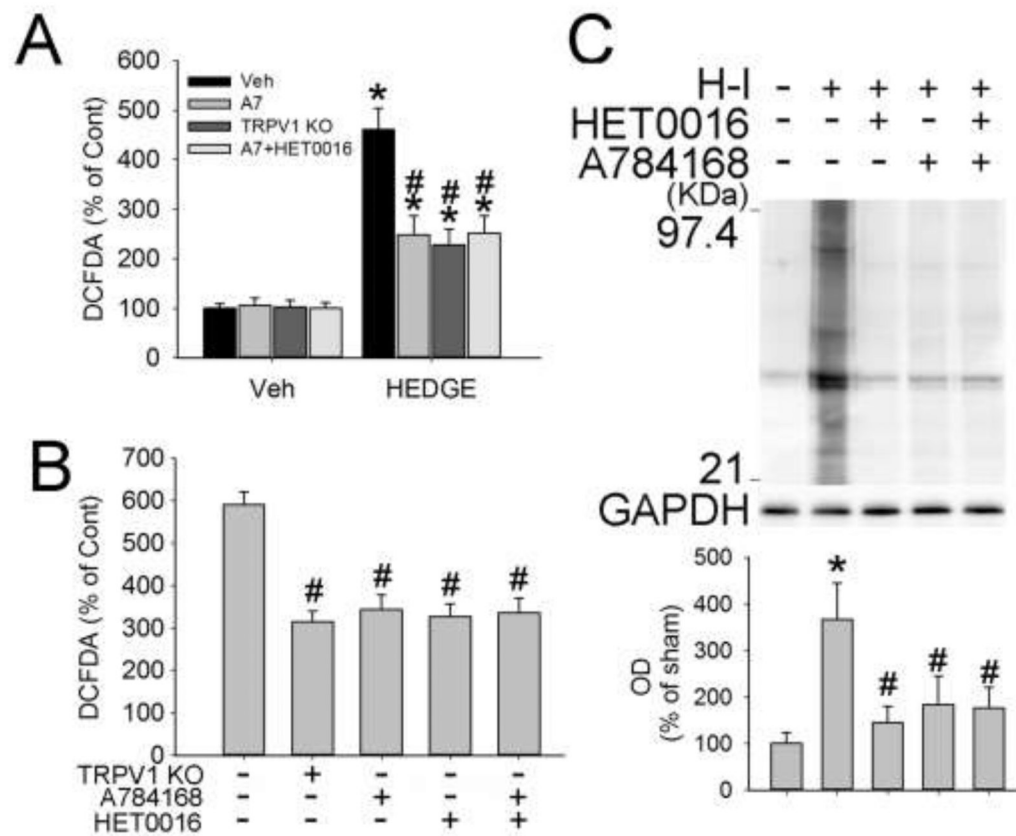


Figure 3. HET0016 and TRPV1 inhibition reduce ROS production. (A, B) TRPV1 knockout (KO), HET0016 and TRPV1 inhibition reduce ROS production. (A, B) TRPV1 knockout (KO), A784168 (A7), and HET0016 each attenuated the ROS production induced by 20-HETE mimetic 20-5,14-HEDGE (HEDGE, A) or 1-h OGD (B), as measured by the presence of 2', 7'-dichlorodihydrofluorescein diacetate (DCFDA). The combination of A784168 and HET0016 did not achieve additive effects. (C) Western blot analysis revealed increased carbonyl immunoreactivity, indicative of H-I-induced oxidative stress, in the ipsilateral hemisphere at 3 h of recovery. HET0016 and A784168 each reduced carbonyl immunoreactivity. The combination of A784168 and HET0016 did not achieve additive effects (n=4-7/group). Optical density (OD; mean \pm SD) was integrated over multiple protein bands (21–97.4 kDa). * p <0.05 vs wild-type+vehicle (Veh)/control procedure; # p <0.05 vs wild-type OGD/H-I+vehicle.

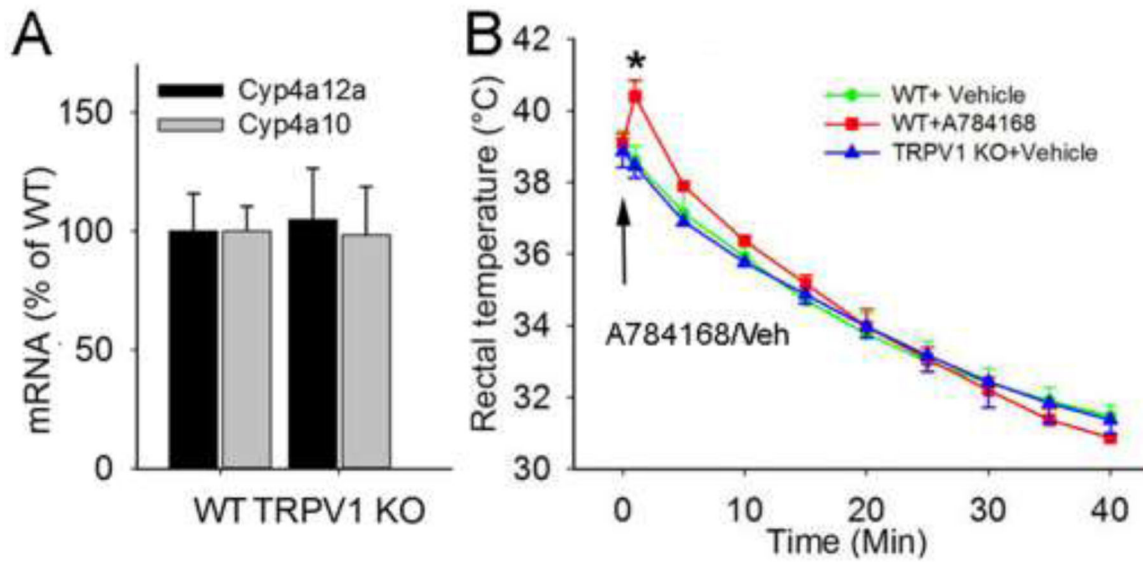


Figure 4.

Effects of TRPV1 on CYP4A mRNA and body temperature. (A) TRPV1 knockout (KO) did not alter levels of neuronal Cyp4a10 or 4a12a mRNA. (B) Anesthetized, 3-month-old TRPV1 KO and wild-type (WT) mice showed comparable baseline temperature and a similar temperature decline without external warming. A784168 (10 $\mu\text{mol/kg}$) caused a transient hyperthermic response, $n = 4/\text{group}$. * $p < 0.05$ vs WT+vehicle (Veh). The arrow indicates the time at which A784168 or vehicle was applied.

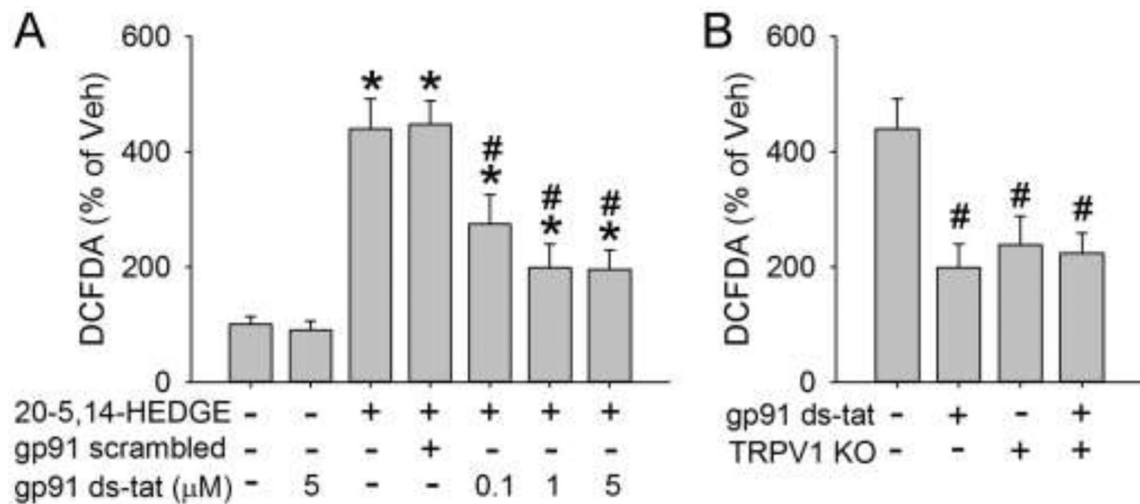


Figure 5.

Effects of TRPV1 and NADPH oxidase 2 (NOX2) on 20-HETE-induced ROS production. (A) The NOX2 inhibitor gp91 ds-tat dose-dependently reduced 20-HETE mimetic-induced ROS production, as measured by the presence of 2',7'-dichlorodihydrofluorescein diacetate (DCFDA). Scrambled gp91 ds-tat was used as a control. (B) TRPV1 knockout (KO) and gp91 ds-tat (5 μM) each attenuated 20-HETE mimetic-induced ROS production but did not exhibit additive effects when combined. * $p < 0.05$ vs vehicle treatment only on wild-type neurons; # $p < 0.05$ vs 20-5,14-HEDGE treatment only on wild-type neurons.